APPLYING PHASE PLANE ANALYSIS TO CEREBROVASCULAR AUTOREGULATION AND PATIENT OUTCOME FOLLOWING BRAIN INJURY

By

COURTNEY ERIN SEMKEWYC

A thesis submitted to the

School of Graduate Studies

Rutgers, The State University of New Jersey

In partial fulfillment of the requirements

For the degree of

Master of Science

Graduate Program in Biomedical Engineering

Written under the direction of

William Craelius

And approved by

_____

_____

_____

_____

New Brunswick, New Jersey

May 2019

ABSTRACT OF THE THESIS

Applying Phase Plane Analysis to Cerebrovascular Autoregulation and Patient Outcome Following Brain Injury

by COURTNEY ERIN SEMKEWYC

Thesis Director:

William Craelius

Cerebrovascular autoregulation (AR) is an important mechanism within the brain that aims to maintain adequate blood flow to all lobes thus promoting proper brain function. Brain injuries due to a traumatic (TBI) or non-TBI event can damage this internal feedback mechanism leading to an impaired response that can lead to secondary injury in the form of swelling or ischemia. This impaired response is reflected in the intracranial pressure (ICP) waveform in the form of varying peak heights, and enlarged valleys. The ICP waveform could be used as a predictive index of patient cerebrovascular autoregulation state, and outcome through the use of integral phase plane analysis and the phase area ration (PAR). PAR is a method of comparing phase plane areas to assign a numerical value to different waveform shapes, and can be calculated through the use of graphical techniques. To test PAR as a predictive index patients were chosen from a database of hemodynamic data and grouped by injury type (TBI or non-TBI), and outcome (rehab or deceased). PAR was able to determine waveform differences

representative of the patient's physiological state not only in terms of injury type, but outcome as well. PAR can be used as a patient-specific predictor of cerebrovascular autoregulation state and patient outcome through the incorporation of the integral phase plane. PAR provides additional patient information that could aid in improving both patient care and management. To further validate these results and feasibility of the index additional testing is required with an increased patient sample size.

Acknowledgements

I would like to thank Dr.Craelius for his tremendous support and guidance throughout this project. Thank you to my thesis committee, Dr.Shinbrot and Dr.Danish for all their help. I would also like to thank Dr.Qadri and the previous members of the Biomechanics and Rehabilitation Engineering Lab for laying the groundwork for this project, and providing me with the necessary patient data and information.

Table of Contents

List of Figures

List of Tables

Introduction

Clinical Problem

Brain injury from a blow to the head or underlying condition is very serious and its treatment requires careful monitoring and precise treatment protocols. Brain injuries are classified as either traumatic (TBI) or non-TBI. In the United States, TBI affects up to 2 million people every year [1]. The traumatic force associated with a TBI can result in primary injuries such as hematomas, contusions, and diffuse injuries [2]. Non-TBI on the other hand is a brain injury that is usually caused by an underlying condition, examples of which include hemorrhage, encephalitis, or vasculitis [3]. Non-TBI injuries are typically researched individually by injury type, and as such there is a lack of information on the occurrence and recovery of this grouping of injuries as a whole. Both TBI and non-TBI injuries result in neuroinflammation of the brain, and can damage the underlying internal mechanisms of the brain including cerebrovascular autoregulation leading to secondary injury [4]. Secondary injury can come in the form of elevated intracranial pressure, or ischemia, which is a lack of oxygen due to impaired or absent blood flow.

Cerebrovascular autoregulation (AR) is the process in which the brain attempts to maintain adequate blood flow throughout all lobes of the brain to promote proper perfusion. AR is a complex process that involves control of blood flow through vasodilation and vasoconstriction, as well as the flow of cerebrospinal fluid (CSF), in an attempt to maintain cerebral perfusion pressure (CPP) and intracranial pressure (ICP) within adequate ranges [5]. Intracranial pressure is the pressure exerted inside the skull, and when elevated causes excess stress on the brain that can increase the severity and likelihood of secondary injury. As a result, most TBI and non-TBI patients are probed for

ICP monitoring during their stay in the hospital. This allows healthcare professionals to monitor the ICP level, and keep it within a safe range. This type of ICP monitoring and management has been associated with a significant decrease in patient mortality [6,7]. Not only is the value of the ICP signal important, but the shape of its waveform also provides key insight into the underlying mechanisms and symptoms of a patient.

Management of ICP in patients with TBI and non-TBI is critical to their recovery. As a result, many researchers are looking into developing a predictive index as a means of better understanding a patient's AR competence through their ICP signal, or even predicting changes in ICP such as hypertensive spikes. This information would allow a physician to provide the best care for a patient, and potentially act prospectively to prevent damage by addressing the problem before it occurs. As a result, many researchers have taken to studying and analyzing clinical patient data as a means of developing a predictive index.

The difficulty of this methodology is that ICP represents the pressure measured within a small volume of parenchyma inside the brain, and cannot be measured in a singular vessel. This results in the ICP being affected by a multitude of different factors and processes within the brain at every given moment. It is extremely difficult to determine an index that will be able to predict a future change in ICP or attempt to understand its meaning as slight alterations in ICP could be caused by a single factor or a combination of these various factors. Most approaches for a predictive index look into the numerical values of the ICP signal, while others look into the shape of the waveform. Some indices look at a comparison with a physiological signal such as arterial blood pressure (ABP) [8]. Others look at the correlation between the amplitude and mean of the

ICP signal [9]. Some have even looked into the differential of the ICP signal in combination with phase plane analysis [10].

There are numerous approaches to ICP analysis that could possibly provide clinically predictive indices of TBI, however none have yielded practical prognosticators of outcome in relation to treatments. There is thus an urgent need for an index that can guide ongoing interventions for maximum efficacy.

Related Work

Prx

Prx is the pressure reactivity index, and is calculated by finding the correlation between the ABP and ICP signals [8]. This index has been found to be somewhat predictive of patient outcome in patients with TBI [8,11]. Prx also creates a U-shaped distribution that can be used to determine the optimal cerebral perfusion pressure (CPP) of a patient. Although, this application is thought to be biased as it is driven to form a U-shaped curve even when using a cross-correlated randomly generated ICP signal proving that it may not be as informative as previously thought [12]. Other studies have found that Prx may fall short of other indices, such as RAP in predicting ICP events [9].

RAP

One index that was able to predict hypertensive spikes in an ICP signal, and can be used monitor patient status is the compensatory reserve index, RAP [9]. RAP is a correlation between the ICP amplitude and mean. The integrity of this index has been called into question due its use of the mean ICP. This is because the mean ICP is

influenced by baseline effect errors. These baseline effect errors can come in the presence of spontaneous shifts in the baseline ICP, or a drift in the signal [13,14]. These baseline errors can cause opposing RAP values when monitoring at different locations within the brain thus bringing its accuracy and reliability into question [14]. As a result of the effect of these errors many people have begun to dismiss RAP, and its effectiveness as an ICP predictive index.

PAR and the Differential Phase Plane

Phase area ratio (PAR) has been proven an effective tool in assessing the smoothness of joint kinetics, and as such could be used compare waveforms through their smoothness in the phase plane [10,15]. This methodology provides a numerical representation of the differences between phase plane curves based on three areas. These three areas are the footprint area (AF), the hull area (AH), and the loop area (AL). AF is the area enclosed by the phase plane curve, AH is the area inside convex hull around the phase plane curve, and AL is the area of any self-intersecting loops [15]. This makes PAR sensitive to peak changes through the corresponding changes in the phase plane especially through changes in the AH and AL.

This technique was paired with the differential phase plane, and found that simulated waveforms with altering amount of peaks (1-3) result in different PAR values [10]. This suggests that PAR could be used as a predictive index through its effectiveness in differentiating between ICP cycles. It was also found that although this method did demonstrate changes based on peak number it could not predict a future hypertensive event in an ICP signal [10].

Predictive Indices

These three predictive indices are just three of the many methodologies that have been attempted in finding a breakthrough index. Unfortunately, the variability and complexity of the physiological mechanisms at work during brain injury make it extremely difficult to find an index that works in most circumstances, and is not affected by baseline errors. The ICP waveform tells a story about these physiological mechanisms, and as such could be the key to developing a predictive index. The potential of this methodology was visited when PAR was able to differentiate between simulated ICP cycles of different peak number.

ICP Waveform

The ICP waveform tells a story of the underlying condition of the brain in a patient, and as such should be further explored as the driving force behind a predictive index. A normal ICP waveform has three distinct descending peaks, known as P1, P2, and P3 (Fig. 1). P1 is the percussion wave that represents the arterial systolic pressure, P2 is the tidal wave that represents the increase in ICP in response to the increase in volume, and P3 is the dicrotic wave that represents the aortic valve closure [16]. A more simplistic way of viewing the first two peaks is that P1 relates to the arterial pulse, and P2 can be thought of as the compliance of the brain [16-19]. These peaks can change in amplitude in response to different physiological conditions such as changes in ICP elevation, or impaired cerebrovascular autoregulation (Fig. 2) [18,20]. Comparing ICP waveforms could provide insight into patient outcome, injury severity, and internal mechanisms.

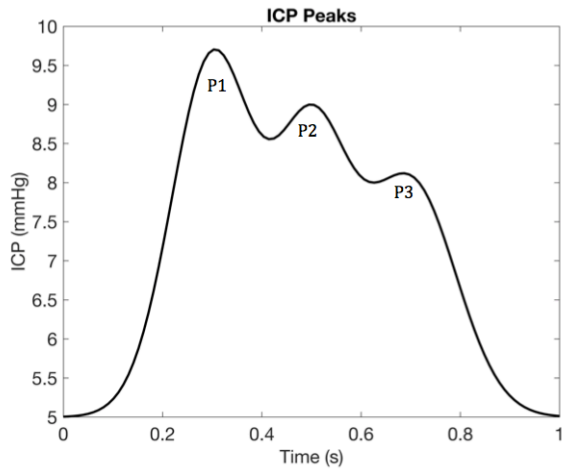

Figure 1: ICP Peaks – ICP curve with the three descending peaks of a normal ICP wave labeled. P1 is the percussion peak and is usually the tallest peak, P2 is the tidal peak, and P3 is the dicrotic peak.

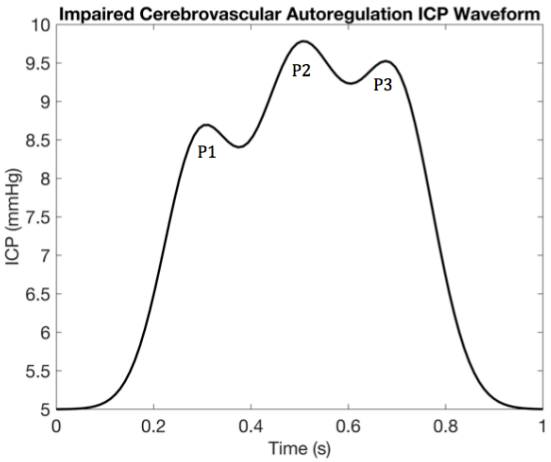

Figure 2: Change in ICP Waveform – Impaired cerebrovascular autoregulation or compliance causes an increase in intracranial volume leading to a spike in the P2 wave [18].

PAR and the Integration Phase Plane

The phase plane curve can be produced using different methodologies such as the signal differential as in the Qadri paper, or the integral phase plane [10]. The differential phase plane tends to emphasize small changes in the ICP shape that could be due to noise, patient movement, or other sources of error. These small changes in ICP result in large loops and jagged curves in the phase plane (Fig. 3C). The integral phase plane on the other hand provides a smoothed ICP curve that is less susceptible to noise, and results in a smoothed phase plane curve thus reducing the effect of error (Fig. 3B). This is due to the fact that the integration phase plane curve is driven more by the ICP waveform as a whole as compared to the small changes in ICP slope, and as such the integral phase plane is used to compare these waveforms. PAR calculated from the integral phase plane could be used as a predictive index to predict patient outcome and state of cerebrovascular autoregulation through the use of phase plane analysis of the ICP waveform.

A) B) C)

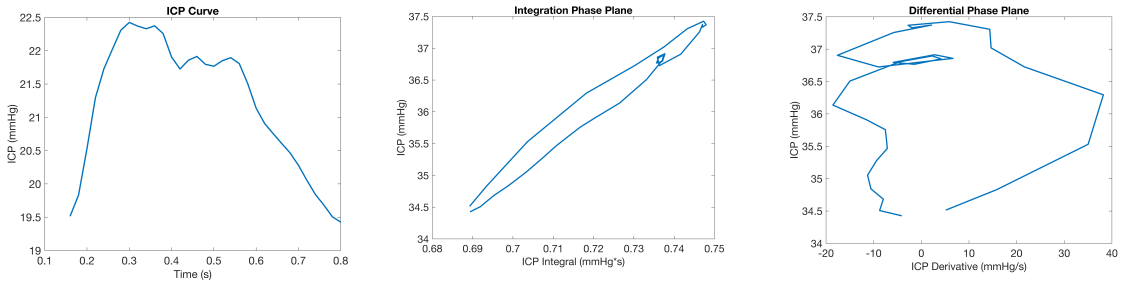

Figure 3: Phase Plane Curve Comparison – A) One cycle of ICP data used to generate the phase plane curves. B) The integration phase plane curve, which focuses more on the ICP waveform as a whole. C) The differential phase plane curve that focuses on the small changes in ICP slope.

Methods

Patient Selection

Patients were selected by the clinical staff at Robert Wood Johnson University Hospital based on the diagnosis of a brain injury. The clinical staff also provided all the demographic information, such as patient age and diagnosis. The data and information collection procedure was approved by the Rutgers University Institutional Review Board (IRB), and follows all HIPAA guidelines.

Signal Collection

This study is a post-acquisition data analysis study that drew from ICP signals in a database, of which the signal collection methodology is outlined in, 'Trending autoregulatory indices during treatment for traumatic brain injury', by Dr.Kim. This paper details that the ICP signals of the selected patients were continuously recorded at a sampling rate of 50Hz either through the use of a bolt or ventriculostomy (*Camino Direct Pressure Monitor, Camino Laboratories,* San Diego, CA) with both methods of data collection requiring a hole to be drilled through the skull of the patient [21]. A bolt also known as a subdural screw is implanted into the subdural space of the brain, while the ventriculostomy is inserted into the lateral ventricle, and can also be used to manage CSF volume through draining [22]. In this study about half the patients received the bolt and the other half the ventriculostomy, but over the past few years the ventriculostomy has become increasingly used as the preferred method of ICP monitoring due to its increased capabilities of CSF management.

The ICP signal along with other vital signals were sent to a clinical monitor that is traditionally used within the SICU, and then exported to a General Electric TRAM-rac 4A [21]. This device is able to both isolate and filter the input vital signals, and output them to a data acquisition device (*NI-USB 6210 DAQ, National Instruments Inc*) from which they are directly sent to an on-site laptop [21]. The patient ICP signals were collected on an hourly basis so that each data file contains a total of one hour of ICP monitoring. All the patient signals were stored in an online database for future use.

Patient Exclusion

The database comprised of a total of 33 patients with brain injuries ranging from subarachnoid hematoma to pituitary tumor. Patients were excluded from this study if there were less than ten recorded ICP signals (less than 10 hours of ICP data), there wasn't enough demographic information on the patients to group them, or there was a problem with their ICP signal or it's recording. An ICP recording problem included signals that were all or a majority noise (Fig.4A). Other patients were excluded based on the shape of their recorded signal, in which the signals had a consistent pulse pressure greater than 10mmHg during each cycle (Fig. 4B). This was removed on the basis that the average pulse pressure of an ICP wave is only 6.1mmHg, and as such these excluded signals did not mimic an ICP signal in terms of shape or value [23]. From the original set of 33 patients, 6 were rejected due to having fewer than ten data files, 2 were rejected for not having enough information to break them into groups, 2 were rejected because the signal was all noise, and 2 were rejected due to having a consistent amplitude difference

greater than 10mmHg. After exclusions 21 patients were left with usable ICP data to be included in this study.

A) B)

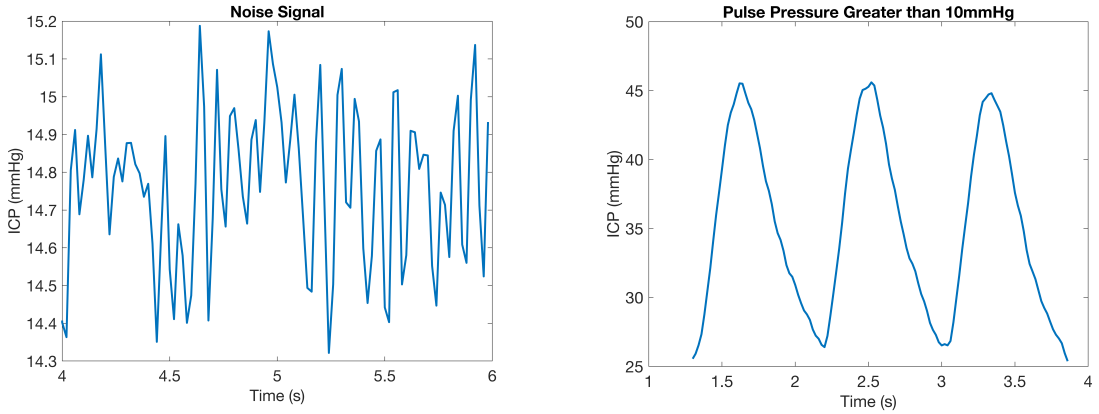

Figure 4: Examples of Excluded ICP Signals – A) Example of an excluded patient ICP signal that was a majority or all noise. B) Example of an excluded patient ICP signal due to having a consistent pulse pressure greater than 10mmHg, which does not mimic the typical ICP behavior.

Patient Grouping

To determine if phase plane analysis can be a predictor of patient outcome and cerebral hemodynamic regulation patient groupings were compared. Patients were grouped by type of injury, and then further by outcome. From the database of patient ICP data two injury type groupings, and two outcome subcategories were created (Fig. 5). The patients were first split into injury categories based on if they had a TBI or a non-TBI. The difference between these two groupings is that the TBI grouping received their injuries due to some sort of traumatic force such as a fall, while the non-TBI group injury

is typically due to an underlying condition that affects the integrity or pressure within the brain.

After this initial split there were 15 patients in the TBI group, and 6 patients in the non-TBI group. These two groups were then further divided by patient outcome. Based on reported patient outcome during their stay in the hospital patients were either grouped into the rehab group or the deceased group. This grouping method resulted in a total of six patient groups: T-group, Tr-group, Td-group, N-group, Nr-group, and Nd-group (Table 1). The T-group consists of all 15 TBI patients, which was then further divided into the Tr-group and Td-group. The Tr-group consists of the 9 TBI patients that went to rehab after their stay in the hospital, and the Td-group consists of the remaining 6 TBI patients that died while in the hospital. The N-group is made up of the 6 non-TBI patients, which then gets further divided into the Nr-group consisting of 5 rehab non-TBI patients, and the Nd-group that only has 1 deceased non-TBI patient (Table 1). Since the Nd-group has only one patient it cannot be compared on its own, and as such is only used as part of the N-group. These five patient categories are used to compare the initial PAR values of patients based not only upon their injury type, but also their outcome.

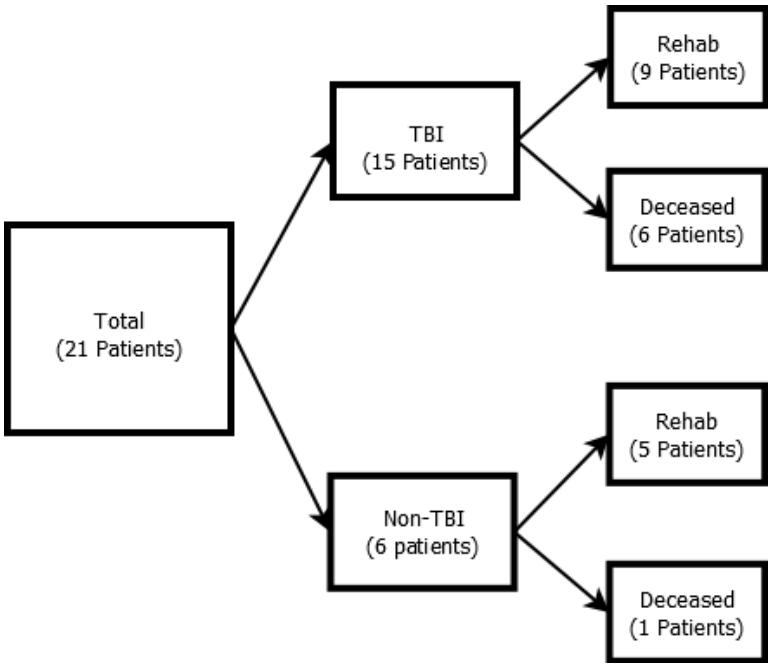

Figure 5: Patient Group Flowchart – A Flowchart demonstrating how the patients were broken into the six patient groups.

Table 1: Patient Groups

Group Description	Group Name	Number of Patients
TBI patients	T-Group	15
TBI patients that went to rehab	Tr-Group	9
TBI patients that are deceased	Td-Group	6
Non-TBI patients	N-Group	6
Non-TBI patients that went to rehab	Nr-Group	5
Non-TBI patients that are deceased	Nd-Group	1

Signal Exclusion

From the database of patient ICP data the first clean signal closest to the admittance of the patient to the hospital was chosen. This was done as a means of determining the initial classification of a patient before the influence of days to weeks of

treatment. Each patient folder contains their ICP signal data file per hour, and starting with the hour of admittance each data file was examined for a clean signal [21]. A clean signal is characterized by a recognizable ICP signal with limited segments of noise alone. After removal of signals it was found that out of the 21 patients, 14 of them had usable signals at admittance, and the other 7 had usable signals within the first 24 hours of being admitted.

Signal Processing

To obtain the most accurate data without the influence of noise the patient ICP signals were filtered. This was done through the use of a Butterworth filter in MATLAB. A Butterworth filter creates an n^{th} order low-pass filter using the desired cutoff frequency and sampling frequency. The Butterworth filter uses a normalized cutoff frequency w_n that corresponds to the cutoff frequency and sampling frequency through Equation 1 [24].

$$w_n = \frac{f_c}{\left(\frac{1}{2} f_s\right)}$$

Equation 1: [24] (1)

This equation determines the normalized cutoff frequency w_n, through the division of the cutoff frequency f_c with half the sampling frequency f_s. This creates an n^{th} order low-pass filter with the desired cutoff frequency.

The sampling frequency f_s used for ICP data collection was 50 Hz making it a constant in Equation 1. As a result, to determine the filter for the ICP data two key parameters needed to be tested. These two parameters were the cutoff frequency and the

order of the filter. First, to determine the cutoff frequency the order was held constant at 5, while the cutoff frequency was adjusted and compared to the original unfiltered signal. Various cutoff frequencies were examined ranging from 4 Hz to 20Hz (Fig. 6A). It can be seen that the lower frequencies over filter the signal leading to the filtered signal not maintaining the general shape of the original unfiltered signal. The higher frequencies on the other hand had a tendency to under filter the data leading to a filtered signal almost identical to the unfiltered data. Previous studies have used a frequency cutoff of 16Hz or 20Hz, but through the comparison of filtered signals with the unfiltered signal it was determined that a cutoff frequency of 16 Hz was better for data analysis as it did not over filter the signal as with the 20Hz cutoff [25,26]. This cutoff frequency allows for the filtered signal to maintain the same shape as the unfiltered signal as to not compromise the signal analysis, while still removing some noise effects.

A) B)

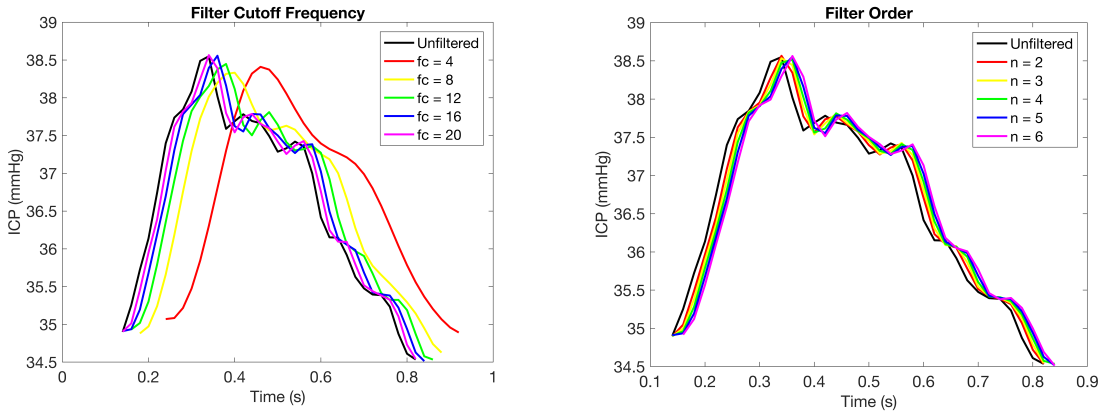

Figure 6: Butterworth Parameters – A) Testing different cutoff frequencies - One cycle of patient ICP data shown as the original signal in black, and the color lines depicting the application of different cutoff frequencies. B) Testing different filter orders – One cycle of patient ICP data shown in black, and the colored lines demonstrating increasing filter orders.

The second filter parameter was the order of the low-pass filter, which determines the roll-off rate [27]. In other words the order determines how quickly the signal is dissipated after the cutoff frequency is reached. Multiple studies have used a 5^{th} order low-pass or Butterworth filter to remove noise from ICP data, but different orders were tested to validate this choice [28-30]. Different orders were tested by keeping the cutoff frequency constant at 16 Hz, and plugging in various orders ranging from 2 to 6. All five orders produced very similar results, but it was visually determined that an order of 5 was able to maintain the dynamical features of the ICP wave (Fig. 6B). This is due to the fact that orders lower than 4 and higher than 5 produced peaks with slightly exaggerated slopes with an order of 5 producing the closest resemblance to the original signal slopes.

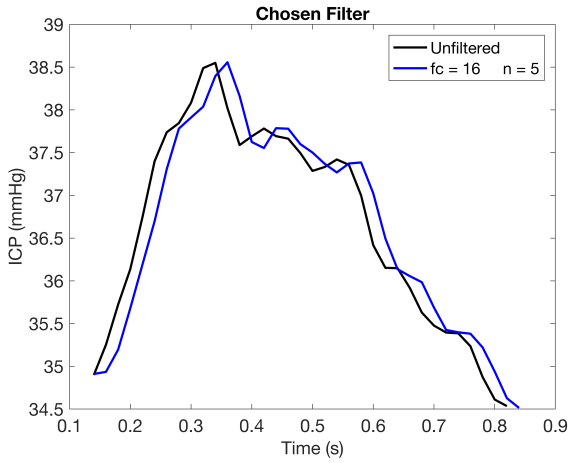

Figure 7: Chosen Filter – The original ICP signal is shown in black compared with the chosen Butterworth filter with f_c=16Hz and n = 5 shown in blue.

Through these two tests it was determined that the best filter for data analysis was a 5^{th} order Butterworth filter with a cutoff frequency of 16 Hz (Fig. 7). This filter produces a filtered signal similar in both shape and value to the original unfiltered signal, while still removing the effect of noise. This filter produces the magnitude bode plot as seen in Figure 8, which depicts both the cutoff frequency and rate of roll-off. This Butterworth filter was used to filter the ICP signals of all the patients.

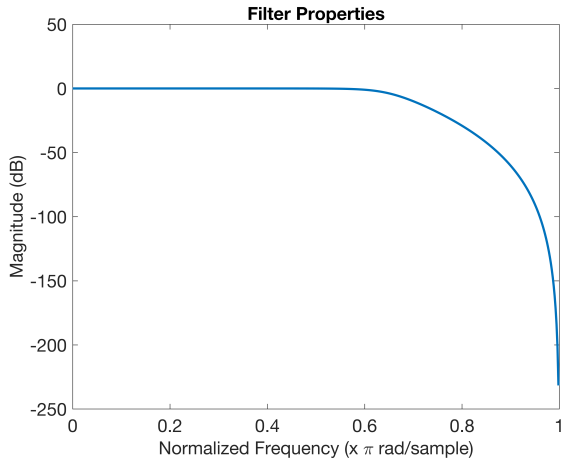

Figure 8: Filter Magnitude Properties – Bode plots showing the magnitude properties of the selected Butterworth filter. The cutoff is set at 16Hz, which appears as 0.64π when converted to a normalized frequency, w_n.

Technical Approach

Integration

Phase plane analysis is used to determine the state of a system, and this was achieved through plotting the integral of the ICP signal against the original ICP signal. The integral phase plane was chosen as the integral of the ICP signal results in a filtered ICP signal. Integration of the ICP signal is the area under the curve of the ICP signal, which results in a smoother ICP signal making it less susceptible to noise, while still maintaining the shape of the ICP signal (Fig. 9A & 9B) [31]. Derivation on the other hand emphasizes all the little peaks and valleys within the ICP signal as it represents the slope of the signal. This method is susceptible to noise and small changes within the ICP signal (Fig. 9A & 9C). As to obtain a more accurate phase plane depiction of the shape of the ICP waveform integration was chosen as the preferred method.

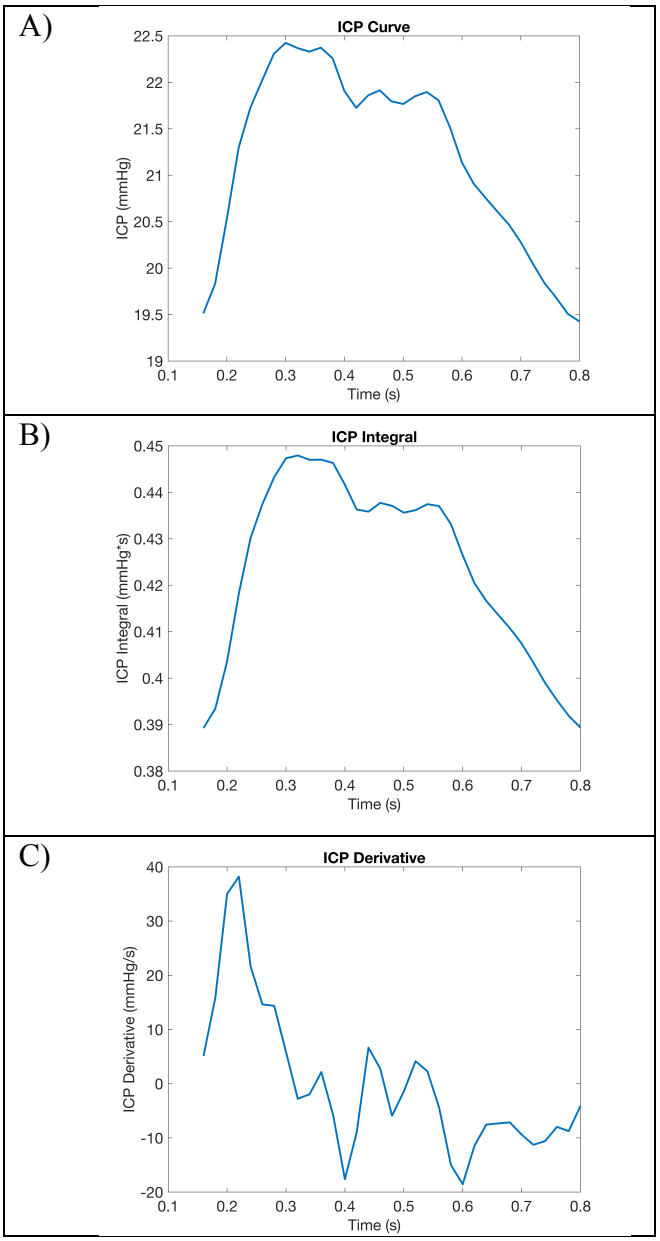

Figure 9: Integration vs. Differentiation – A) One cycle of collected ICP data from a patient B) The integral of the ICP data seen in part A, and can be seen as a smoothed copy of the original ICP data. C) This is the derivative of the original ICP data in part A, and emphasizes even the small peaks and valleys seen in this signal.

Since the integration phase plane was the chosen state of the system the trapezoidal rule was used to obtain the ICP integral (Equations 2 and 3). The trapezoidal

rule uses the input of a signal or function, and is able to generate the integral by creating various small trapezoids under the curve that represent the area [32]. The equation then calculates and sums the area of these trapezoids to determine the integral of the curve. In the case of the ICP signal the trapezoidal rule takes the input of the ICP curve and integrates it over time.

Trapezoidal rule

Equation 2: $$\Delta x_i = x_i - x_{i-1}$$ [32] (2)

Equation 3: $$\int_a^b f(x)dx = \frac{\Delta x_i}{2}\sum_{i=1}^{N} f(x_{i-1}) + f(x_i)$$ [32] (3)

In these two equations x is replaced by the time t, f(x) is replaced by the value of the ICP signal, i is a sub-interval that determines what time and ICP point is utilized, and N is the highest required value of i. Equation 2 determines the width of the trapezoid by determining the difference between two time points, which is then input into Equation 3. Equation 3 finds the area of the trapezoid by taking the width and multiplying it by the height, or difference in ICP points.

To obtain the most accurate integration of the signal adjacent time and ICP points were used. This means that every trapezoid has a width of 0.02 seconds, and each ICP cycle contains anywhere from twenty to forty trapezoids. These trapezoidal rule equations were implemented into MATLAB code to automatically generate the integrated ICP signal (Fig. 10). The results of this code can be seen in Figure 9B.

```
%Integral
%Using the Trapezoidal Rule
velocityb = zeros(1,length(cycleb));
for i = 2:length(cycleb)
dx = time_sb(i)-time_sb(i-1);
velocityb(i) = sum(((cycleb(i-1)+cycleb(i)).*(dx./2)));
end
```

Figure 10: Trapezoidal Rule MATLAB Code - In this code, velocityb represents the integral of one ICP waveform, or one cycle of the input ICP signal, which is represented by the variable cycleb.

Phase Area Ratio (PAR)

The phase plane curve in this experiment is one ICP cycle plotted against the integral of that same ICP cycle (Fig. 11A). Another way to think of this is the ICP curve plotted against the area under the ICP curve, and is a visual representation of changes within the shape of the ICP waveform. The phase plane depicts the state of a function over a period of time, and the phase area ratio is the numerical representation of the phase plane areas. These areas are the phase footprint area (AF), which is the area comprised within the phase plane curve (Fig. 11B). The second area is the loop area (AL), which is the area of any loops created by the phase plane curve (Fig. 11C). The final area is the hull area (AH) that is the area enclosed by the tightest-fit convex hull around the phase plane curve (Fig. 11D). An example of a phase plane curve, and the corresponding regions that each of these areas encloses can be seen in Figure 11. To obtain the elliptical phase plane curves and a more accurate PAR value the first integral and ICP cycle point of each signal were removed as outliers.

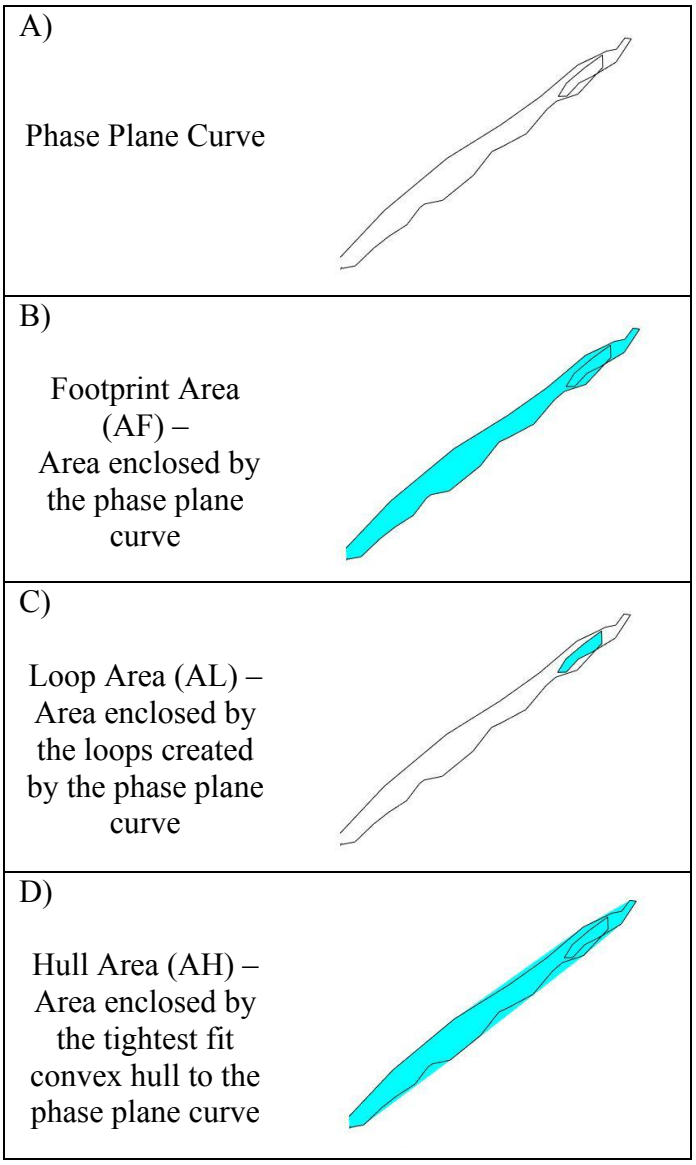

Figure 11: PAR Parameters – A) The phase plane curve created by plotting the ICP curve against its integral. B) The footprint area is the area enclosed within the phase plane curve including any loops. C) The loop area is the area of any loops and nested loops created by the phase plane curve. The nested loop areas are counted multiple times, according to their order (i.e., first loop, second loop, etc.) D) The hull area is the area enclosed by the tightest fit convex polygon to the phase plane curve. The phase plane curve outline can be seen in black, and the enclosed region by a phase plane area is in cyan.

Using these areas the phase area ratio can be calculated through the use of Equation 4 [15]. ICP curves that do not follow a typical waveform will result in a higher PAR as they will have an increase in both hull and loop area. A sine wave results in a perfect PAR of zero, and as such the more similar in structure the ICP curve is to a sine wave the lower the PAR value. This means that ICP waveforms that have distinctive peaks and valleys with large amplitude differences will result in a higher PAR, and tend to be associated with a worse state of cerebrovascular autoregulation and compliance.

Equation 4: $$PAR = 1 - \frac{AF}{AL + AH} \quad [15] \quad (4)$$

PAR is the ratio of area within the phase plane curve (AF) to the sum of the area of the loops (AL) with the area of the convex hull (AH).

To get a more accurate PAR value for each patient three PAR values were computed at different time points for the ICP signal. These time points are at the beginning, middle, and end of the signal. Since ICP signals are collected and stored on an hourly basis these time points correspond to their position within an hour. So the beginning PAR value is calculated within the first few minutes, while the end PAR value is calculated in the final few minutes of that hour. These three PAR values were then averaged to obtain the final PAR value for each patient.

Footprint Area (AF) and Hull Area (AH) Calculation

From Equation 4 it can be seen that PAR is dimensionless and as such a graphical solution can be used to calculate the value of PAR without finding the numerical value of each region. This can be done in MATLAB by plotting the phase plane curve, and then determining the number of pixels located within each region. Finding the ratio of pixels per region is equivalent to determining the ratio between the actual areas of each region. This method allows for the use of MATLAB image processing tools to convert the phase plane graph into a black and white binary image from which the number of black pixels filling the area of a specified region can be determined (Figs. 12 & 13). This method allows for a simplistic calculation of areas of any shape, size, and location in pixels. MATLAB imaging techniques shown in Figure 12 for the hull area were also used to determine the areas of the footprint and loops.

```
%AH calculation
k = convhull(velocityb,cycleb);
figure
fill(velocityb(k),cycleb(k),'k','LineWidth',2);
axis = gca;
axis.Visible = 'off';
saveas(gca,'Power4.png')
ahBW = imread('Power4.png');
ahb = im2bw(ahBW,0.5);
totalPixelsAH = numel(ahb);
WhitePixelsAH = sum(ahb(:));
BlackPixelsAH = totalPixelsAH - WhitePixelsAH;
harea = BlackPixelsAH;
AH = harea;
```

Figure 12: MATLAB Hull Area Calculation – Piece of MATLAB code that utilizes MATLAB image processing tools to determine the number of pixels captured within an area.

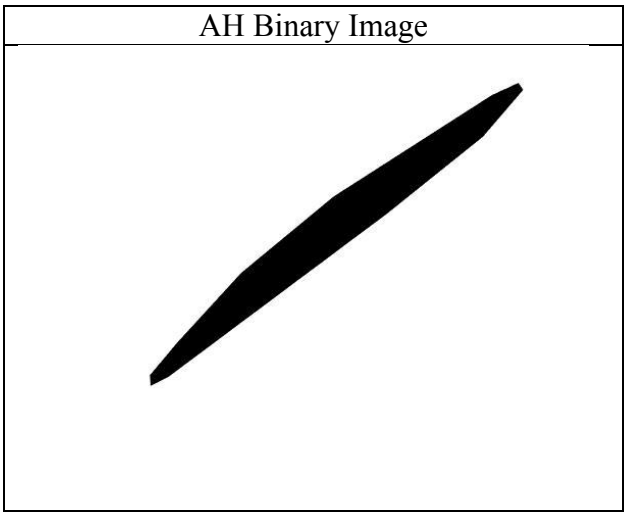

Figure 13: Binary Hull Area – Binary image of the hull area of a phase plane curve.

The MATLAB code used to determine the number of pixels in an area is done by first filling the plot of the desired area of the phase plane curve, or convex hull. Next, is to save the filled in plot as an image without the axes as to avoid their influence on the number of pixels. MATLAB then has a function im2bw that converts an image into a black and white binary image so that everything that was filled in appears in a matrix as a 0, and the rest of the open space appears as a 1 (Fig.13). So in this case the black 0 pixels are representative of the area that needs to be calculated. To determine the number of black pixels, the number of white pixels was subtracted from the total number of pixels leaving the area of the region in question. This process was done for each of the three PAR regions to determine the space they fill in terms of pixels that was then plugged into the PAR equation (Equation 4).

Loop Area (AL) Calculation

The code and process for determining the area of the loops and nested loops involved additional processes as compared to the AF and AH calculations. For these two areas the phase plane curve or the convex hull could be filled in to determine its area. This could not be done for the loops using a simple MATLAB built in tool as it did not permit the nested loops to be calculated individually thus causing the AL to be underestimated. To solve this problem a series of code was used that ran through the phase plane curve point by point looking for an intersection point [33]. This intersection point is the first point at which the curve intersects with itself thus creating a loop. The developed code then removes all the points outside the loop, and determines the area of the first loop in the same manner as AF and AH by converting it to a binary image and counting the black pixels. Once this is complete the code removes the loop points from the curve thus generating a new phase plane curve minus the first loop, and begins to look for the next intersection point. This process continues until all the loops are accounted for.

Normal ICP Curve Simulation

As a method of visually and numerically comparing the patient groups to a normal healthy ICP curve a simulated normal ICP curve was generated. This curve was simulated through a combination of Gaussian curves, as discussed in the paper, ‘Phase Plane Analysis & Morphological Simulation of Intracranial Pressure Variability for Physiological Monitoring of Acute Severe Brain Injury’ by Dr.Qadri.

Equation 5: $$ICP_{SIM} = A_1 e^{-B_1(t-C_1)^2} + A_2 e^{-B_2(t-C_2)^2} + A_3 e^{-B_3(t-C_3)^2} + D \quad [10] \ (5)$$

This equation adds three Gaussian curves together to create one wave with three peaks. The amplitude of these peaks is determined by A, the width by B, the location relative to zero by C, and the baseline ICP by D [10]. The time vector was represented by t, and was a vector of 100 points from 0 to 1 second. The parameters listed in Table 2 are similar to that of the Qadri paper, and were used to create this normal ICP wave simulation. The combination of these parameters results in the ICP curve and phase plane curve depicted in Figure 14.

Table 2: Normal ICP Simulation Gaussian Parameters [10]

Parameter	Value
A_1	4.6
B_1	75
C_1	0.3
A_2	3.5
B_2	90
C_2	0.5
A_3	3
B_3	60
C_3	0.7
D	5

Statistical Testing

A two-tailed student's t-test with an alpha value of 0.05 was performed when comparing patient groups as a method to determine if the group PAR results were statistically significantly different from one another.

Results

Simulated ICP

An ICP curve was simulated to establish a baseline PAR value that would represent an ideal by which to quantify the impaired groups. The control ICP waveform contained three distinct peaks in descending order starting from the first peak or percussion wave (Fig. 14A). The height and widths of these peaks in a normal ICP curve can vary, but the waveform maintains the same general shape. As expected, the phase plane that resulted from the control-simulated signal was a smooth ellipse with two small inner loops (Fig. 14B). The smoothness of the ellipse causes the AL and AH values to be almost identical leaving the PAR value to rely mostly on the small AL value. Since, AL is a small number compared to that of AF and AH this causes the PAR to be very small coming in at 0.039 for this simulated normal signal.

A) B)

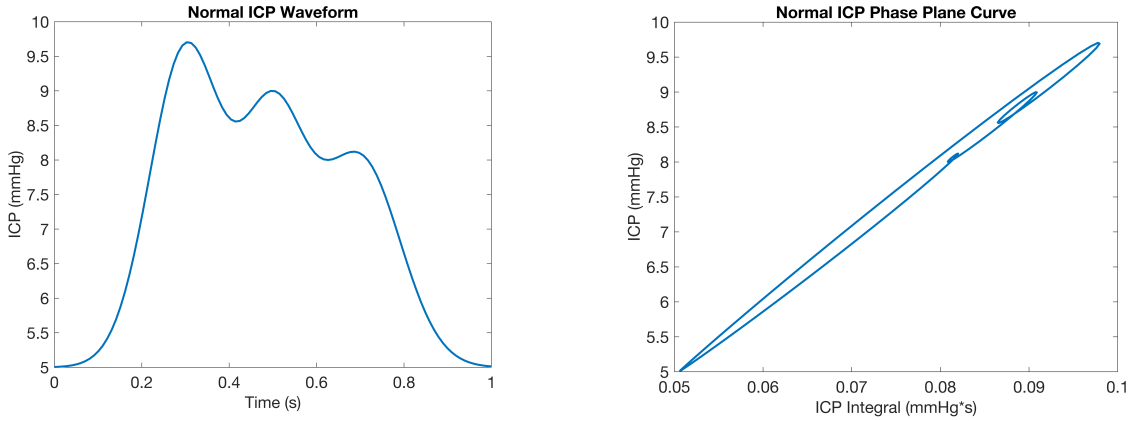

Figure 14: Normal ICP Curve – A) A simulated normal ICP waveform generated from the addition of three Gaussian curves. B) The phase plane curve generated from the simulated normal ICP curve.

Visual Findings

The three main groups are the Tr-group, Td-group, and the Nr-group. This is due to the fact that the Tr-group and Td-group comparison compares ICP curves and phase plane curves based on patient outcome. The Nr-group makes up a grand majority of the N-group, and as such is a good representation of that group. Through the plotting of the ICP curves and phase plane curves of these three groups visual differences can be seen.

The general trend of the Tr-group (TBI patients that went to rehab) seen in a majority of patients, but not all is an ICP curve that has three or more small peaks across the top (Fig. 15A). This tends to mimic the ICP curve of a healthy individual that typically has a curve with three small descending peaks (Fig. 14A & 15A). The phase plane curve generated from this data results in an elliptical curve with no loops to a few small loops (Fig. 15B).

A) B)

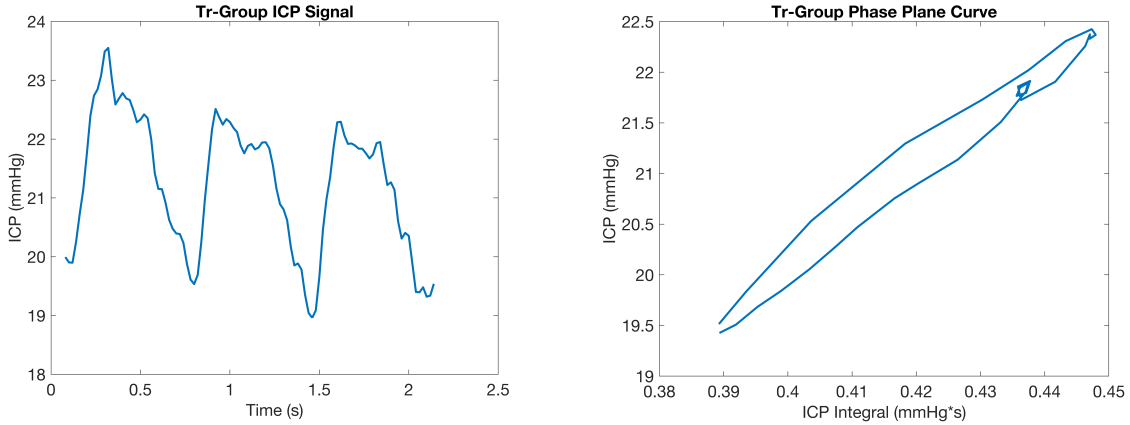

Figure 15: Tr-Group Representation – A) Three ICP cycles taken from a patient in the Tr-group as a representation of a majority of the ICP signals within this group. B) The phase plane generated by a single cycle of the ICP signal from the same patient used in part A.

The general trend of the Td-group (deceased TBI patients) is the presence of a large notch between the percussion and tidal peaks (Fig. 16A). The large valleys generated between the three peaks, especially between the percussion and tidal peaks causes a phase plane curve with an increased number of loops. The loops in the Td-group vary in both shape and size, and can lead to indents in the elliptical shape of the phase plane curve (Fig. 16B).

A) B)

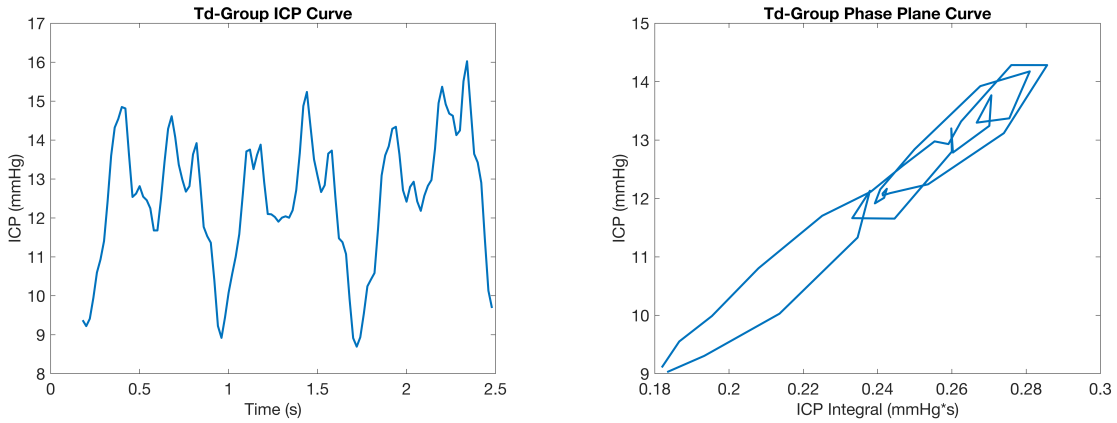

Figure 16: Td-Group Representation – A) Three cycles of ICP data taken from a patient in the Td-group that is representative of the majority of ICP signals in this group. B) The phase plane curve that originates from integrating one cycle of ICP data from this same patient and plotting it against the ICP.

The Nr-group (non-TBI rehab patients) has an ICP waveform with an enlarged tidal peak, which typically signifies poor intracranial compliance and increased intracranial volume (Fig.17A) [18]. This heightened tidal peak is followed by a cascade of smaller peaks leading to most of the waveforms having greater than three peaks similar

to that of the Td-group. The large tidal peak results in a large loop in the phase plane curve, which may be accompanied by a few smaller loops (Fig.17B).

A) B)

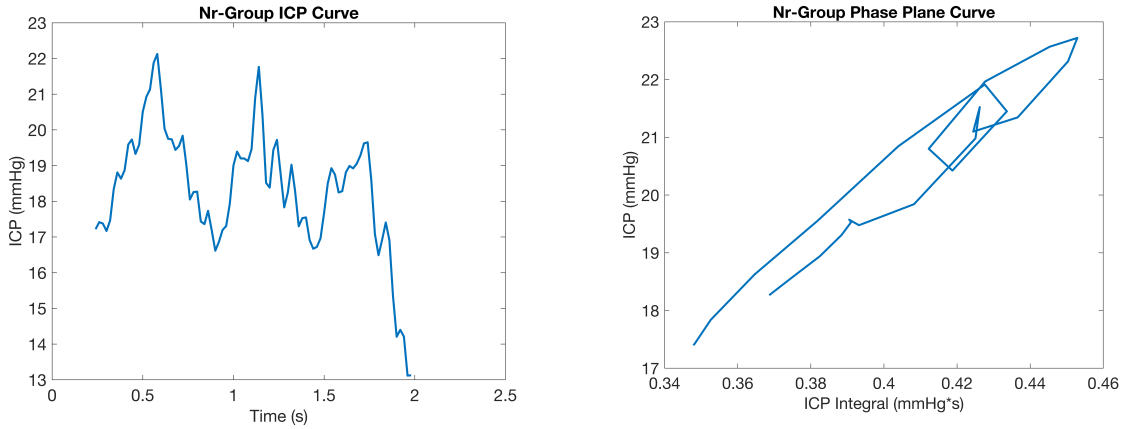

Figure 17: Nr-Group Representation – A) Three cycles of ICP data taken from a patient in the Nr-group that is representative of some patients in the Nr-group. B) The corresponding phase plane curve generated from one cycle of ICP data taken from this same patient in the Nr-group.

For all three groups the ICP waveform shape varied from patient to patient, but the repeated trends seen in multiple patients in a single group are depicted as the group representations above.

Numerical Findings

The phase planes of these three groups, and their corresponding PAR values (Tr, Td, and Nr) reflected their ICP curves as expected; corresponding PAR values are seen in Table 3. The smooth quality of the ellipse of the phase plane curve accompanied by the few small loops leads to the Tr-group having the smallest PAR value at an average value of 0.16. The large notch and valleys in the Td-group causes a multitude of loops of

varying shapes and sizes, which explains the fact that this group has a higher average PAR value at 0.23. Combining the Tr-group and Td-group into the T-group that represents all the TBI patients leads to a mean PAR value of 0.19. This value is smaller than the mean PAR of the six non-TBI patients that was 0.25. This can be explained by the fact that the non-TBI patients have a shorter period with a greater amplitude difference between smaller peaks as compared to the larger period with a smaller amplitude difference between peaks as seen in the TBI patients. Finally, the Nr-group had a mean PAR of 0.26, which made up a grand majority of the N-group data.

Table 3: Group Results

Group	N	Mean PAR	Standard Deviation
T	15	0.19	0.066
Tr	9	0.16	0.049
Td	6	0.23	0.066
N	6	0.25	0.018
Nr	5	0.26	0.018

Legend: T – all TBI patients, Tr – TBI patients that went to rehab, Td – TBI patients that are deceased, N – all non-TBI patients, Nr – non-TBI patients that went to rehab

To determine if there are differences between these patient groupings a two-tailed Student's t-test was performed. This test was performed comparing two groups at a time. To compare the phase plane curves of patients based upon their outcome the Tr-group and Td-group were selected, and it was determined that these two groups are statistically significantly different (Table 4). Then moving to the category of injury type the Tr-group

was compared to the Nr-group, and the T-group was compared to the N-group. Both of these tests found a p-value of less than 0.05 with an alpha value of 0.05 demonstrating that they are significantly statistically different as well (Table 4).

Table 4: Group Comparison

Group	Comparison Group	p-value
Tr	Td	0.030
	Nr	0.023
T	N	0.028

Discussion

The results of this study demonstrate that there are differences in ICP waveforms and their corresponding integral phase plane between patients based upon their type of injury and outcome. The differences in patient ICP waveform cause different phenomena in the phase plane, such as a heightened tidal peak leading to a large loop in the phase plane (Fig. 17B). PAR is a means of taking these physiological differences in ICP (Figs. 15A, 16A & 17A), and assigning it a numerical value.

The ICP signal of the Tr-group (Fig.15A) held the closest resemblance to that of a normal ICP signal (Fig. 14A). This visual finding is mimicked by the fact that a normal ICP signal produces a similar phase plane curve (Fig. 14B & 15B) with a nice elliptical shape, and small inner loops. The ICP simulation also produced a PAR of 0.039, and it should be noted that an ICP curve would never produce a perfect PAR value of zero, as this can only be done by a sinusoidal wave due to its absence of peaks. The presence of the peaks is what defines an ICP curve, and what will always lead to a PAR value greater than zero. As such, the ideal PAR value for a patient is around 0.039.

The Tr-group having the smallest PAR value of the groups at an average value of 0.16, and can be explained by its similarity to the normal ICP curve. The ICP curve of the Tr-group is similar to that of the normal ICP curve with a few small descending peaks near the top signifying that their systems are running close to normal, and that there are no concerns of poor compliance or hypertensive events. The Tr-group in the phase plane typically has a pretty smooth ellipse like the normal ICP curve, but with a slightly greater indent meaning that the AF and AH pixel numbers are very similar leading to a greater

influence of AL on PAR. The combination of the slight difference between AF and AH paired with the small AL leads to a lower PAR value.

The Td-group on the other hand has an average PAR value of 0.23, and is due to its more erratic shape, and increased number of loops. The increased number of loops for this group tends to cause the elliptical shape of the phase plane curve to have sudden bulges and indents leading to more space between the perimeter of the phase plane and the convex hull, leading to a larger difference between AF and AH (Fig. 16B). The increased amount of loops also causes an increase in AL, and paired with the smaller ratio of AF to AH results in a higher PAR value. The Nr-group has an average PAR of 0.26, and can be explained by its similarities to the Td-group in having a larger AL, and smaller ratio of AF to AH (Fig. 17B).

The large tidal peak seen in both the Td-group and Nr-group signifies that the compliance of the brain has decreased as the volume has increased, and the cerebrovascular autoregulatory system has failed to make the proper adjustments to account for these changes. These adjustments include changing the resistance, and the displacement of both CSF and venous blood from the affected area [18]. The decrease in compliance forces the percussion peak to decrease, while the tidal peak increases, as does the volume of blood (Fig. 2).

Since the PAR value of the rehab patients is greater than that of the normal ICP simulation it demonstrates that these patients have impaired cerebrovascular autoregulation or decreased compliance as a result of their condition. Functional cerebrovascular autoregulation and proper compliance within the brain would result in proper blood flow and pressure throughout the brain resulting in a normal ICP waveform.

As a patient recovers their compliance and cerebrovascular autoregulation should begin to return to normal thus causing their ICP waveform to alter in shape beginning to more closely resemble that of the normal ICP waveform. This means that the higher the PAR value the more abnormal the ICP shape, and the worse the condition and outlook for the patient.

The Td-group and Nr-group tend to have an ICP curve with an increased number of peaks, and large valleys in between these peaks (Fig. 16A & 17A). This trend results in a higher PAR value as it causes an increased number of loops and size of these loops within the phase plane. The similarities between the ICP waveforms and their phase plane curves demonstrate that type and severity of injury are very important factors that affect the ICP of a patient. The Td-group had a TBI accompanied by a poor outcome, but still had a lower PAR value than the Nr-group patients that had a non-TBI accompanied by a better outcome. A non-TBI injury can affect the brain differently than a TBI injury explaining this finding.

The fact that non-TBI patients have a higher PAR value corresponds with a study conducted in 2008 on 172 patients comparing TBI and non-TBI patients based on injury type and severity that found that TBI patients had a lower disability rating, and higher scores on both motor and cognitive tests as compared to the non-TBI group [3]. These findings demonstrate that TBI patients tend to have a better recovery than non-TBI patients upon hospital discharge. This means that when comparing patients of similar age and injury severity the non-TBI tends to have a more negative impact on the brain and body than a TBI. This observation is also reflected in the PAR values found in this study, as non-TBI patients have a PAR greater than both TBI patient groupings. Since a higher

PAR correlates with an ICP waveform that is increasingly abnormal as compared to a normal ICP curve this means that non-TBI patients tend to have a more abnormal ICP waveform that corresponds to their condition. Non-TBI patients also had a small standard deviation of only 0.018 signifying that their PAR values are all very similar even though they have different diagnoses.

The fact that there is a statistically significant PAR difference (Table 4) based on patient outcome is a very important finding as it supports the use of PAR as a predictive index in the case of TBI. Having a predictive index that can be assessed upon patient admission, and give an idea of patient outcome allows for the healthcare professionals to prepare and respond accordingly. As can be seen in Table 3 the higher PAR values of TBI patients corresponds to an outcome of death, and the lower PAR values are seen in a patient being sent to rehab upon discharge. So higher PAR values could correspond to a higher severity of injury, while the lower PAR values represent less severe injuries. PAR could be combined with other assessment tools such as the Glasgow Outcome Scale (GOS) to obtain a better understanding of patient injury. This would allow patients to not only be assessed by their physical symptoms, but by the state of their ICP waveform as well. Combining this type of internal and external physiological parameters would help to obtain a larger picture of the state of the patient's health, and the likelihood of their recovery.

Having this information could be beneficial to providing adequate care to a patient. A healthcare professional can find the PAR value of a patient upon admission, and use this metric to help determine the type of care this patient needs. This could help to answer questions such as: Does the patient require more surveillance or additional

resources? Should they be placed in a different unit or department? These are important questions when managing the care of a patient, and can help the department to distribute their resources in the best possible fashion.

Injury difference is also an important criterion to determine as it helps to further explain and divide the range of PAR values. If PAR were to be used as a predictive index there would need to be a cutoff that separates patient outcome. This value would be somewhere in between the PAR values of the Tr-group and the Td-group, and might fall around the average PAR of the T-group as a whole. This cutoff may be functional for the TBI patients, but not for the non-TBI patients knowing that the non-TBI patients demonstrate a higher PAR. This can be seen when comparing the average PAR of the Tr-group of 0.16 and the average PAR of the Nr-group at 0.26. Both groups have the same outcome, but the different type of injury caused the Nr-group to have an elevated PAR value. The difference between injury types can also be seen in the comparison between the T-group with a PAR of 0.19 and N-group with a PAR of 0.25. This further iterates the fact that TBI and non-TBI injuries affect the brain and its ICP signal in different ways.

Future Work

This methodology needs to be perfected and validated using a larger sample size as currently the sensitivity and specificity are not at clinical standards. Both the sensitivity and specificity are 0.67 when the T-group average is used as the threshold between patient outcomes. When the threshold value is changed to 0.21 upon observation the sensitivity holds at 0.67, but the specificity rises to 0.89. A larger data pool will have more accurate sensitivity and specificity values, and may even result in different values.

This study was conducted using the ICP signals from 21 patients, which was the amount of usable patients from our database, but ultimately was only a small sample size. The next step of this study would be to obtain the ICP signals on or about admission into the hospital of many more patients. It is hard to confirm or deny the use of PAR as a predictive index with such a small pool as outliers tend to skew the results. A larger data pool would allow for adequate representation of the abilities, usability, specificity, and sensitivity of PAR as a predictive index. This would also allow PAR ranges to be specified for each patient grouping that would be used to predict the outcomes of new patients.

Other than additional patients, additional information would also be useful to obtain better patient groupings. The information used in this study was patient outcome upon discharge from the hospital. The outcome of these patients once they entered rehab is unknown, and would provide important information that could explain patients in the rehab group that had PAR values higher than the average. Having the GOS score of these patients while in the hospital and rehab would allow for better division of patients into groups, and provide better insight into PAR values. This additional information and an

enlarged sample size could also allow the study to account for patient age and injury severity, which could both, affect PAR values.

The final consideration for any future work would be to assess different indices that look into waveform shape, or phase planes. PAR does a good job of finding a numerical representation of the ICP shape. With this in consideration the ICP waveform of the Tr-group varies greatly from that of the Td-group yet their average PAR values are only different by 1.45 times, which doesn't leave much room for error. Finding a wider gap between group averages would allow for a better range, and generate less overlap and outliers. Ultimately, this would produce more accurate results, and lead to an enhanced predictive index with a higher sensitivity and specificity.

Conclusion

This study looked to explore the use of phase plane analysis as a predictive index to assess patient outcome and physiological condition. The integral phase plane was determined as the most effective as it was susceptible to the least amount of noise and smoothed the ICP curve. The phase plane curve obtained by plotting this ICP integral against the original ICP curve allowed for the application of the phase area ratio (PAR) calculation. PAR provided a numerical value for differences in ICP waveform shape in different patient groupings characterized by both outcome (rehab or deceased) and injury type (TBI or non-TBI).

PAR was able to effectively demonstrate these waveform abnormalities with a higher value, and as such found statistically significant differences between various groups. It is notable that the Tr-group was different than the Td-group demonstrating the ICP and PAR differences associated with patient outcome. The Tr-group average was also different than the Nr-group average, and the T-group was different than the N-group showing that non-TBI and TBI injuries don't affect ICP in the same manner. PAR has been shown to be a possible predictive index for clinical application, but to prove its effectiveness additional testing with an increased sample size must first be conducted.

References:

[1] Lenzlinger, P. M., Morganti-Kossmann, M., Laurer, H. L., & Mcintosh, T. K. (2001). The Duality of the Inflammatory Response to Traumatic Brain Injury. *Molecular Neurobiology,24*(1-3), 169-182.

[2] Hawthorne, C., & Piper, I. (2014). Monitoring of Intracranial Pressure in Patients with Traumatic Brain Injury. *Frontiers in Neurology,5*.

[3] Cullen, N. K., Park, Y., & Bayley, M. T. (2008). Functional recovery following traumatic vs non-traumatic brain injury: A case-controlled study. *Brain Injury,22*(13-14), 1013-1020. doi:10.1080/02699050802530581

[4] Kinoshita, K. (2016). Traumatic brain injury: Pathophysiology for neurocritical care. *Journal of Intensive Care,4*(1). doi:10.1186/s40560-016-0138-3

[5] Werner, C., & Engelhard, K. (2007). Pathophysiology of traumatic brain injury. *British Journal of Anaesthesia,99*(1), 4-9. doi:10.1093/bja/aem131

[6] Dawes, A. J., Sacks, G. D., Cryer, H. G., Gruen, J. P., Preston, C., Gorospe, D., . . . Ko, C. Y. (2015). Intracranial pressure monitoring and inpatient mortality in severe traumatic brain injury. *Journal of Trauma and Acute Care Surgery,78*(3), 492-502. doi:10.1097/ta.0000000000000559

[7] Farahvar, A., Gerber, L. M., Chiu, Y., Carney, N., Härtl, R., & Ghajar, J. (2012). Increased mortality in patients with severe traumatic brain injury treated without intracranial pressure monitoring. *Journal of Neurosurgery,117*(4), 729-734. doi:10.3171/2012.7.jns111816

[8] Kirkness, C. J., Mitchell, P. H., Burr, R. L., & New29ell, D. W. (2001). Cerebral Autoregulation and Outcome in Acute Brain Injury. *Biological Research For Nursing,2*(3), 175-185. doi:10.1177/109980040100200303

[9] Pineda, B., Qadri, M. .., Kosinski, C., Kim, N., Danish, S., & Craelius, W. (2015). Developing a Continuous Hemodynamic Autoregulation Monitor. *2015 41st Annual Northeast Biomedical Engineering Conference (NEBEC)*. doi:10.1109/nebec.2015.7117187

[10] Qadri, M. (2017). Phase Plane Analysis & Morphological Simulation of Intracranial Pressure Variability for Physiological Monitoring of Acute Severe Brain Injury (Doctoral Dissertation). Available from ProQuest Dissertations and Theses database.

[11] Sorrentino, E., Diedler, J., Kasprowicz, M., Budohoski, K. P., Haubrich, C., Smielewski, P., . . . Czosnyka, M. (2011). Critical Thresholds for Cerebrovascular Reactivity After Traumatic Brain Injury. *Neurocritical Care,16*(2), 258-266. doi:10.1007/s12028-011-9630-8

[12] Kelly, S., Bishop, S. M., & Ercole, A. (2018). Statistical Signal Properties of the Pressure-Reactivity Index (PRx). *Acta Neurochirurgica Supplement Intracranial Pressure & Neuromonitoring XVI,*317-320. doi:10.1007/978-3-319-65798-1_62

[13] Hall, A., & O'Kane, R. (2016). The best marker for guiding the clinical management of patients with raised intracranial pressure—the RAP index or the mean pulse amplitude? *Acta Neurochirurgica,158*(10), 1997-2009. doi:10.1007/s00701-016-2932-z

[14] Eide, P., Sorteberg, A., Meling, T. R., & Sorteberg, W. (2014). The effect of baseline pressure errors on an intracranial pressure-derived index: Results of a

prospective observational study. *BioMedical Engineering OnLine,13*(1), 99. doi:10.1186/1475-925x-13-99

[15] Wininger, M., Krasner, A., Kim, N. H., & Craelius, W. (2018). Phase plane quantification of single-joint smoothness. *Journal of Biomedical Engineering and Informatics,4*(1), 40. doi:10.5430/jbei.v4n1p40

[16] Ellenbogen, R. G., Sekhar, L. N., & Kitchen, N. D. (2018). *Principles of neurological surgery*. Philadelphia, PA: Elsevier.

[17] Abraham, M., & Signal, V. (2015). Intracranial pressure monitoring. *Journal of Neuroanaesthesiology and Critical Care,2*(3), 193-203. doi:10.4103/2348-0548.165039

[18] Hirzallah, M. I., & Choi, H. A. (2016). The Monitoring of Brain Edema and Intracranial Hypertension. *Journal of Neurocritical Care,9*(2), 92-104. doi:10.18700/jnc.160093

[19] Aboy, M., Mcnames, J., Thong, T., Tsunami, D., Ellenby, M., & Goldstein, B. (2005). An Automatic Beat Detection Algorithm for Pressure Signals. *IEEE Transactions on Biomedical Engineering,52*(10), 1662-1670. doi:10.1109/tbme.2005.855725

[20] Marcus, H. J., & Wilson, M. H. (2015). Insertion of an Intracranial-Pressure Monitor. *New England Journal of Medicine,373*(22). doi:10.1056/nejmvcm1406460

[21] Kim, N., Krasner, A., Kosinski, C., Wininger, M., Qadri, M., Kappus, Z., . . . Craelius, W. (2015). Trending autoregulatory indices during treatment for traumatic brain injury. *Journal of Clinical Monitoring and Computing,30*(6), 821-831. doi:10.1007/s10877-015-9779-3

[22] Khalili, H., Sadraei, N., Niakan, A., Ghaffarpasand, F., & Sadraei, A. (2016). Role of Intracranial Pressure Monitoring in Management of Patients with Severe Traumatic Brain Injury: Results of a Large Level I Trauma Center in Southern Iran. *World Neurosurgery,94*, 120-125. doi:10.1016/j.wneu.2016.06.122

[23]Behrens, A., Lenfeldt, N., Qvarlander, S., Koskinen, L., Malm, J., & Eklund, A. (2012). Are intracranial pressure wave amplitudes measurable through lumbar puncture? *Acta Neurologica Scandinavica,127*(4), 233-241. doi:10.1111/j.1600-0404.2012.01701.x

[24] Butter. (n.d.). Retrieved from https://www.mathworks.com/help/signal/ref/butter.html

[25] Kashif, F. M., Verghese, G. C., Novak, V., Czosnyka, M., & Heldt, T. (2012). Model-Based Noninvasive Estimation of Intracranial Pressure from Cerebral Blood Flow Velocity and Arterial Pressure. *Science Translational Medicine,4*(129). doi:10.1126/scitranslmed.3003249

[26] Bezerra, T. A. (2018). Preliminaryes studies of variability of intracranial pressure in military personnel undergoing combat tactics training in Brazilian air force. *Aeronautics and Aerospace Open Access Journal,2*(5). doi:10.15406/aaoaj.2018.02.00058

[27] Podder, P., Hasan, M. M., Islam, M. R., & Sayeed, M. (2014). Design and Implementation of Butterworth, Chebyshev-I and Elliptic Filter for Speech Signal Analysis. *International Journal of Computer Applications,98*(7), 12-18. doi:10.5120/17195-7390

[28] Piper, I. R., Miller, J. D., Dearden, N. M., Leggate, J. R., & Robertson, I. (1990). Systems analysis of cerebrovascular pressure transmission: An observational study in head-injured patients. *Journal of Neurosurgery,73*(6), 871-880. doi:10.3171/jns.1990.73.6.0871

[29] Stettin, E., Paulat, K., Schulz, C., Kunz, U., & Mauer, U. M. (2011). Noninvasive intracranial pressure measurement using infrasonic emissions from the tympanic membrane. *Journal of Clinical Monitoring and Computing,25*(3), 203-210. doi:10.1007/s10877-011-9297-x

[30] Van Den Brule J., Stolk, R., Vinke, E. J., Loon, L. M., Pickkers, P., Hoeven, J. G., . . . Hoedemaekers, C. W. (2018). Vasopressors Do Not Influence Cerebral Critical Closing Pressure During Systemic Inflammation Evoked by Experimental Endotoxemia and Sepsis in Humans. *Shock,49*(5), 529-535. doi:10.1097/shk.0000000000001003

[31] Jerri, A. J. (1985). *Introduction to integral equations with applications*. New York: Dekker.

[32] Wong, S. S. (1997). *Computational Methods in Physics and Engineering*(2nd ed.). Singapore: World Scientific Publishing.

[33] NS (2009). Curve Intersections, MATLAB Central File Exchange. Retrieved February 18, 2019.